Publishing House
AKAPIT

COMPUTER METHODS IN MATERIALS SCIENCE
Informatyka w Technologii Materiałów

Vol. 15, 2015, No. 1

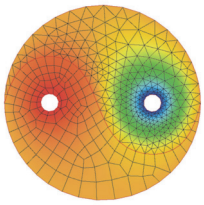

NUMERICAL INVESTIGATION OF REFILL FRICTION STIR SPOT WELDING JOINTS

ANNA DERLATKA*, PIOTR LACKI

Czestochowa University of Technology, Dąbrowskiego 69, 42-202 Częstochowa, Poland
**Corresponding author: aderlatka@bud.pcz.czest.pl*

Abstract

The paper presents an analysis of tensile tests for welded specimens made of 6061-T6 aluminium alloy. Three kinds of lap joins were made by Refill Friction Spot Stir Welding (RFSSW). The each specimen has one joint, but they were varied in the position of the sheets. In the first, the angle between sheets axes was 0º, to determine the tensile capacity of the joint. In the second and third, the angle between sheets axes was 20º, and -20º. That position of sheets allow determine the maximum load and displacement of stretched and twisted structure. The numerical calculations were performed using the ADINA System based on the Finite Element Method (FEM). The sheets and joints were modelled with 3D-solid elements. The experimental investigations were carried out using a testing machine and a non-contact and material independent measuring system providing, for loaded test objects, accurate 3D displacements and surface strain values. The stress, strain distribution and displacements were analysed. The numerical and experimental results were compared. The structures were assessed in respect of strength and the possibility of applying in the aircraft industry.

Key words: finite element method, aluminium 6061-T6, Refill Friction Spot Stir Welding (RFSSW)

1. INTRODUCTION

Friction Stir Welding (FSW) is used in automobile and aircraft structures in order to reduce weight and improve performance in relative to the rivets. The process is characterized by reliability and low time-consuming preparation of materials for welding and making the joint. FSW competes with traditional linear welding methods such as TIG-welding (Lacki & Derlatka, 2013; Lacki et al., 2012) Refill Friction Stir Spot Welding (RFSSW) and other methods (e.g. riveting and hybrid joints presented by Sadowski et al. (2013), Sadowski and Golewski (2013), Sadowski et al. (2011) belong to a group of modern spot joining techniques.

RFSSW is used for welding aluminium alloys i.e. AA 6061-T6 (Venukumar et al., 2013), AA2024-T3 and AA5754-H22 analysed by Bozkurt and Bilici (2013) because of the good quality of the joints, especially in comparison to traditional welding techniques. It is also possible to join other materials e.g. titanium (Kudła et al., 2009), steel (Sun et al., 2014; Ghosh et al., 2011) or steel with aluminium alloy (Kundu et al., 2013). The continuous and smooth face of the RFSSW joint is formed by a specific tool consisting of a probe, sleeve and clamping ring (figure 1). In Mishra and Mahoney (2007) is presented,

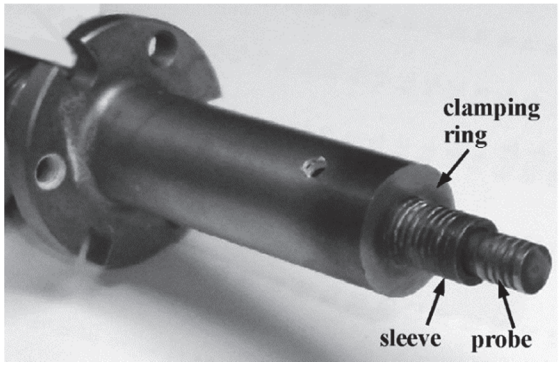

Fig. 1. *Tool for Friction Stir Spot Welding process.*

ISSN 1641-8581

that the sleeve and probe are the moving parts which can rotate and protrude for heating and plasticization of the base material. Yuan et al. (2011) present the analyze of the spots making by two tools: a conventional tool with a center pin and an off-center feature tool.

finite elements: full shell elements model, full 3D-solid elements model and 3D-solid and shell elements model for analysis the structures during tensile testing. The full 3D-solid model is the most exact, but it requires a long total solution time. The alternative for shorter computational and modelling times are 3D-shell elements. In Fanelli et al. (2012) the RFSSW joints and heat affected zone are

Table 1. *Chemical composition of 6061 aluminium alloy.*

Element content, % wt.									
Cr	Cu	Fe	Mg	Mn	Si	Ti	Zn	other	Al
0.04-0.35	0.15- 0.40	0.70	0.80-1.20	0.15	0.40-0.80	0.15	0.25	0.15	rest

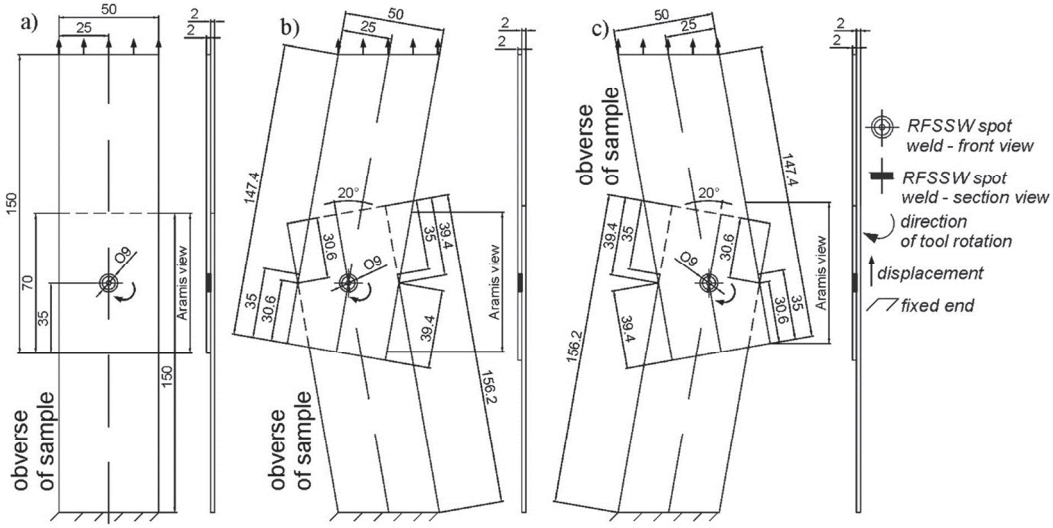

Fig. 2. *Geometry of samples: angle between sheets axes of 0° (a), angle between sheets axes of 20° (b), angle between sheets axes of -20°, mm (c).*

The thermo-mechanical models are used to analyze the welding process. Thermal analyses use a heat source distributed over the tool surface, with a heat flux per unit area. In another approach, the heat input may be distributed over the probe volume. The consequence of the effect of metal flow on the distribution of heat generation is ignored. Assidi et al. (2010) simulate FSW for the Al 6061 aluminum using an Arbitrary Lagrangian Eulerian (ALE) numerical model and a Eulerian formulation, which provides a faster way to reach a steady welding state. To calculate the plastic energy and to account for the change in the yield strength with welding temperature, the model based on welding energy is proposed by Hamilton et al. (2009). A fully coupled thermo-mechanical model presented by Zhang and Zhang (2009) is adopted to analyse the effect of welding parameters: the rotating speed, the welding speed and material flow patterns. To analyse the structures made using RFSSW, the mechanical model is used. Derlatka et al. (2014) present the comparison of three types of model with different kinds of modelled as 3D-sold elements and base material as shell elements. Derlatka and Kasza (2014a, 2014b) present the analysis of bending beams. Complex aluminium structures are made from sheets welded with spot joints. The joints are meshed by 3D-sold elements and sheets by shell elements.

2. GOAL AND SCOPE OF WORK

The analysis of the tensile test results for different configurations of sheets in RFSSW joints is the goal of the paper. The structures were assessed according to tensile strength, strains and displacements. Two sheets of 6061-T6 aluminium alloy are welded as lap joints by RFSSW. The chemical composition of the base material is given in table 1.

Three variants of sheet position relative to each other are analysed – figure 2. In each model, the same finite elements are used: 3D-solid for the RFSSW joint and shell elements for the sheets. The numerical results are compared with experimental investigations. The tensile tests were carried out

using a testing machine and a non-contact optical 3D deformation system, Aramis, which enables measuring displacements and strains.

The RFSSW processes were carried out using the following parameters: joint thickness 2.2 mm, tool rotational speed 2000 rpm, tool input speed 0.7 s, tool output speed 0.5 s.

3. EXPERIMENTAL INVESTIGATION

Figure 3 shows the analyzed samples. Figure 4 shows the force - displacement diagram during tensile tests. The maximum force for the sample with the angle between sheets axes of 0º is 9.8 kN, for the sample with the angle between sheets axes of 20º is 9.2 kN, while for the sample with the angle between sheets axes of -20º is 7.8 kN. The displacements are respectively 1.36 mm, 2.70 mm and 3.58 mm.

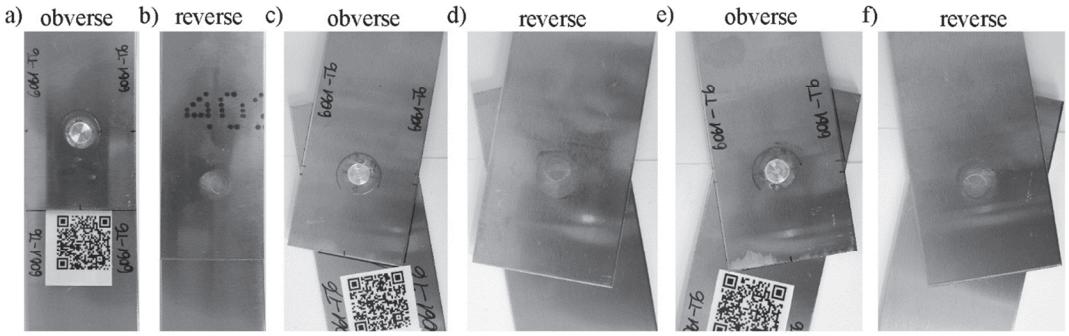

Fig. 3. Analyzed samples: angle between sheets axes of 0º (a-b), angle between sheets axes of 20º (c-d), angle between sheets axes of -20º (e-f).

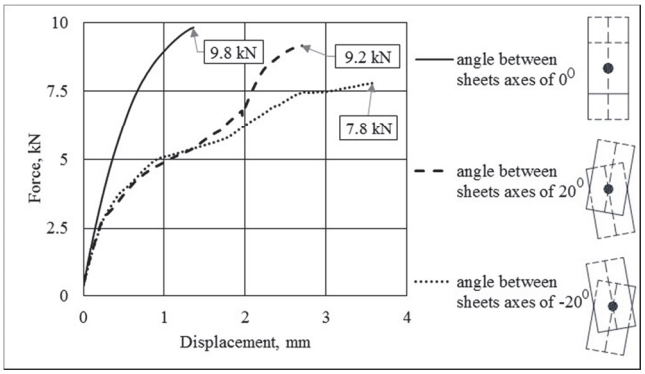

Fig. 4. Force - displacement diagram.

The strain distributions for the analysed samples, during peak force, are presented in figure 5. In each sample, the area of maximum values concentration is located on the edge of the joint and base material. In the first sample, the distributions are symmetrical with respect to the vertical axis (Y-axis). In the samples for the angle between sheets axes of 20º and -20º, the distributions reflect the shape of a screw. The same dependencies are observed in the joint shapes after breaking (figure 6).

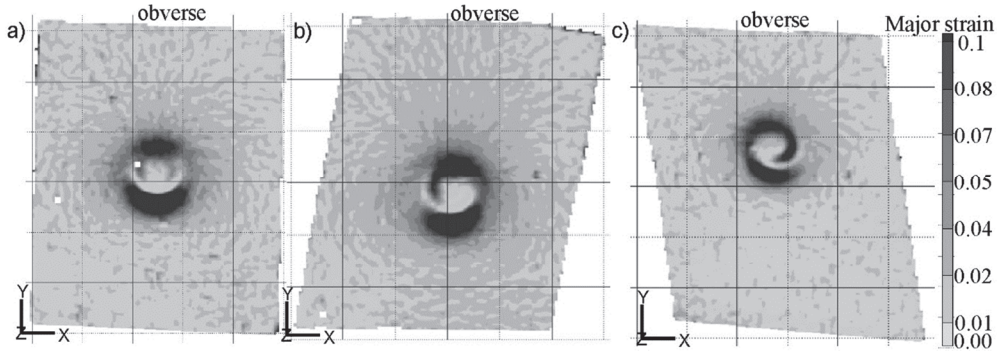

Fig. 5. Strain distribution for samples during tensile test: for angle between sheets axes of 0º (a), for angle between sheets axes of 20º (b), for angle between sheets axes of -20º (c).

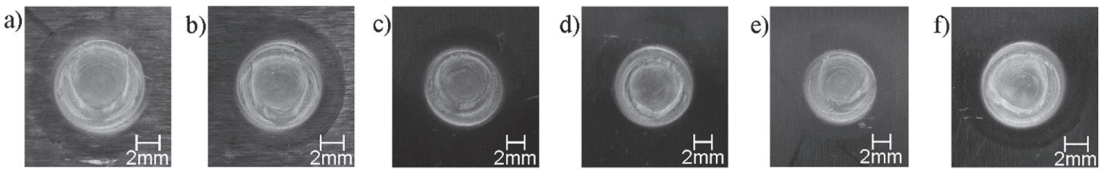

Fig. 6. Joints after tensile test: angle between sheets axes of 0º (a-b), angle between sheets axes of 20º (c-d), angle between sheets axes of -20º (e-f).

4. COMPUTATIONAL MODELS

The ADINA System based on the Finite Element Method was used for the numerical studies. The geometry of the models is identical to the real samples. The model for the samples with the angle between sheets of 1600 do not include the differences in the direction of welding. The sheets and joints are modelled as 8-node 3D-solid elements. Between the 3D-solid element surfaces of the sheets, contact conditions are assumed. The sheet and joint elements are connected in nodes.

perimental value. The meshes of the samples are shown in figures 7, 8.

Plastic orthotropic material with the following parameters: modulus of elasticity 68.9 GPa, yield strength 276 MPa, Poisson's ratio 0.33 and density 2700 kg/m^3, is used for each model.

The model with the angle between sheets of 1800 has 11648 3D solid elements and 15041 nodes. The model with the angle between sheets of 1600 has 9704 finite elements and 12185 nodes. The calculations are performed in 100 time steps.

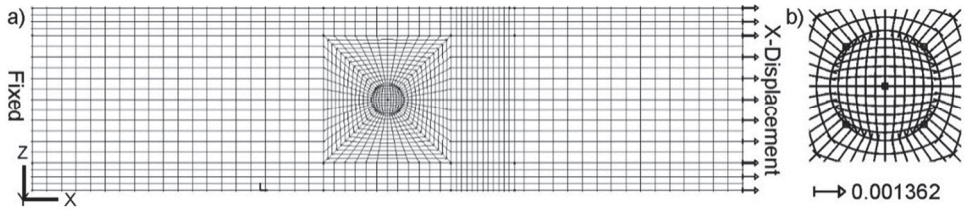

Fig. 7. *Mesh of sample for angle between sheets axes of 0°: whole model (a), RFSSW joint, m (b).*

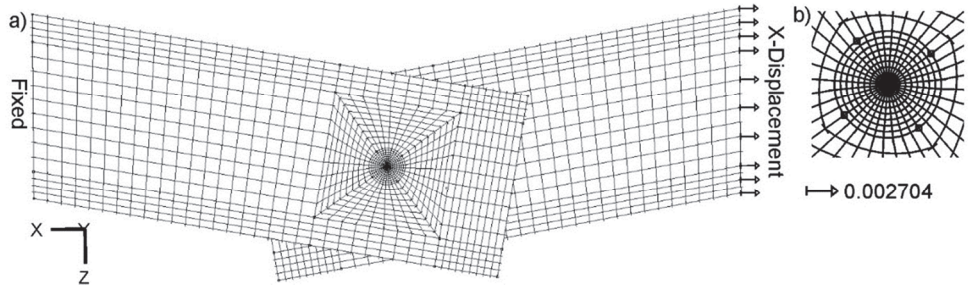

Fig. 8. *Mesh of sample for angle between sheets axes of 20°: whole model (a), RFSSW joint, m (b).*

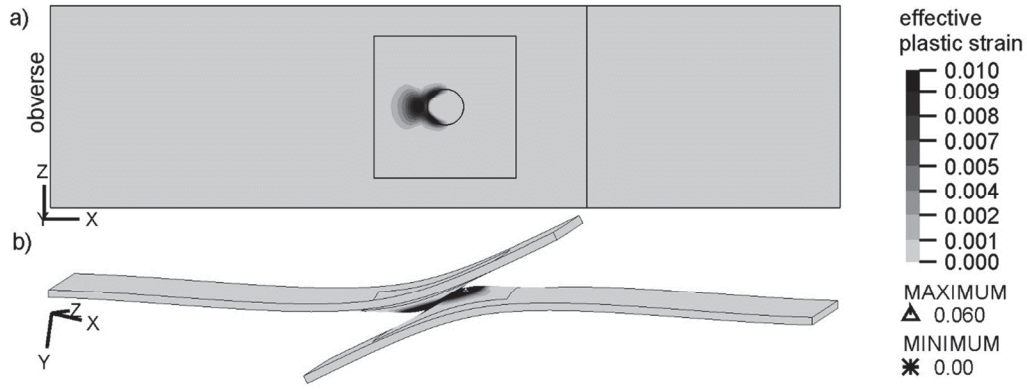

Fig. 9. *Effective plastic strain for sample with angle between sheets axes of 0°: X-Z view (a), axonometric view, mag. 5x (b).*

The boundary conditions and type of load are the same for each sample and they are added to the surfaces. All the degrees of freedom on the first external edge of the sample are fixed, the second external edge has one free degree of freedom (X-translation). This edge is loaded by the displacement of the ex-

5. RESULTS

The effective plastic strains for the sample with the angle between sheets axes of 0º are presented in figure 9. Figure 10 shows the effective plastic strains for the sample with the angle between sheets axes of 20º. The results for the sample with the angle be-

tween sheets axes of -20º are not shown. The strain distributions are similar in the sample with the angle between sheets axes of 20º. Only the extreme results are different.

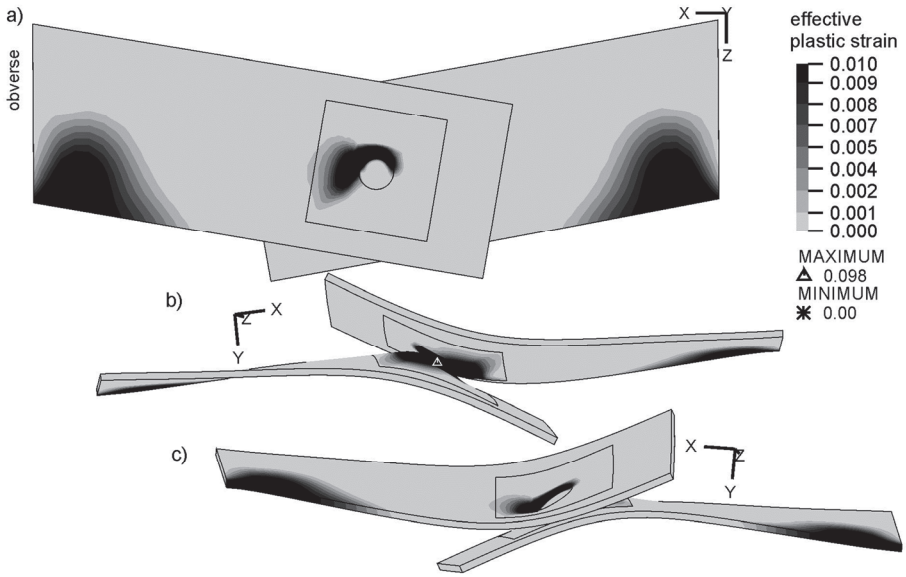

Fig. 10. *Effective plastic strain for sample with angle between sheets axes of 20º: X-Z view (a), axonometric view, mag. 5x (b-c).*

In the sample with the angle between sheets axes of 0º, the effective plastic strain distributions are symmetrical with respect to the X-axis and similar in both sheets. The extreme results are located on the inner sides of the sheets, which is difficult to specifically identify. The maximums are on the fixed part of the sheet, the minimums are on the free part of the sheet. The free parts of the sheets are deflected with respect to the Y-axis.

In the sample with the angle between sheets axes of 0º the strain distributions are not symmetrical, but they are similar in both sheets. The extremes are on the area surrounding the RFSSW joint. The precise location of the extreme results is difficult, because extremes are also located on the inner sides of the sheets and the sheets are asymmetrically deflected.

6. DISCUSION

Based on the displacement-force diagram, the highest breaking force is for the sample with the angle between sheets axes of 0º. The shape of the curve suggests the sample strains during pure tensile. The samples with the angle between sheets axes of 20º are stretched and twisted. Therefore, the curves have a complex shape and the displacements reach higher values.

The structures behaviour affect the places of strain concentration. The numerical studies show that in each sample the maximum value of strains are on the inner part of the joint. In the tensile test, the samples fracture in the RFSSW joint but they do not separate from the sheets.

The sheet Y-displacement for the sample with the angle between sheets axes of 0º are the result of non-fixed edges with respect to the Y-axis. The Y-displacement of the sample with the angle between sheets axes of 20º is caused by the complex behaviour of the sample.

7. CONCLUSION

The analysis of RFSSW joints with a different arrangement of sheets was conducted. The following conclusions were made:

- The strength of the sample with the angle between sheets axes of 0º is higher than the sample with the angle between sheets axes of 20º and -20º.
- In each sample, the maximum strains are observed on the joint area, on the inner surfaces of the sheets. The concentration of strains on the outer surface are observed on the edge of the joint.
- In each case, the fractures are in the joint. The spot welds do not separate from the sheets.
- The sheets of the sample with the angle between axes of two parts of 0º are deflected with respect to the Y-axis. The sheets of the sample with the angle between axes of two parts of 20º are deflected with respect to the Y-axis and they are twisted.

ACKNOWLEDGMENT

Financial support of Structural Funds in the Operational Programme - Innovative Economy (IE OP) financed from the European Regional Development Fund - Project "Modern material technologies in aerospace industry", Nr POIG.01.01.02-00-015/08-00 is gratefully acknowledged.

REFERENCES

Assidi, M., Fourment, L., Guerdoux, S., Nelson, T., 2010, Friction Model for Friction Stir Welding Process Simulation: Calibrations from Welding Experiments, *Int J Mach Tool Manu*, 50, 143–155.

Bozkurt, Y., Bilici, M.K, 2013, Application of Taguchi Approach to Optimize of FSSW Parameters on Joint Properties of Dissimilar AA2024-T3 and AA5754-H22 Aluminum Alloys, *Mater Design*, 51, 513–521.

Derlatka, A., Kasza, P., 2014a, Numerical Analysis of Aluminium Cellular Beams with Cells of Different Diameters, *Adv Mat Res*, 1020, 151–157.

Derlatka, A., Kasza, P., 2014b, Numerical Analysis of Aluminum Cellular Beams with Cells of Different Arrangement, *Adv Mat Res*, 1020, 158–164.

Derlatka, A., Kudła, K., Makles, K., 2014, Numerical Analysis of RFSSW Joints, *Proc. Conf. 11th World Congress on Computational Mechanics*, eds, Oñate, E., Oliver, X., Huerta, A., Barcelona, Spain, 6807–6816.

Fanelli, P., Vivio, F., Vullo, V., 2012, Experimental and Numerical Characterization of Friction Stir Spot Welded Joints, *Eng Fract Mech*, 81, 17–25.

Ghosh, M., Kumar, K., Mishra, R.S, 2011, Friction Stir Lap Welded Advanced High Strength Steels: Microstructure and Mechanical Properties, *Mat Sci Eng A-Struct*, 528, 8111–8119.

Hamilton, C., Sommers, A., Dymek, S., 2009, A Thermal Model of Friction Stir Welding Applied to Sc-Modified Al–Zn–Mg–Cu Alloy Extrusions, *Int J Mach Tool Manu*, 49, 230–238.

Kudła, K., Wojsyk, K., Lacki, P., Śliwa, R., 2009, Zgrzewanie Tarciowe Stopów Tytanu z Aluminium, *Inżynieria Materiałowa*, 5, 306–309 (in Polish).

Kundu, S., Roy, D., Bhola, R., Bhattacharjee, D., Mishra, B., Chatterjee, S., 2013, Microstructure and Tensile Strength of Friction Stir Welded Joints between Interstitial Free Steel and Commercially Pure Aluminium, *Mater Design*, 50, 370–375.

Lacki, P., Adamus, J., Sadowski, T., Wojsyk, K., Kneć, M., 2012, Experimental and Numerical Analysis of the Tensile Test of Aluminium Welded Samples, *Proc. Conf. European Congress on Computational Methods in Applied Sciences and Engineering 2012*, eds, Eberhardsteiner, J., Böhm, H.J., Rammerstorfer F.G., Vienna, Austria.

Lacki, P., Derlatka A., 2013, The Application of FSW Technology in Aluminium Structures, *Met Form*, 24, 205–218.

Mishra, R.S, Mahoney, M.W, 2007, *Friction Stir Welding and Processing*, ASM International, Materials Park, Ohio.

Sadowski, T., Balawender, T., Śliwa, R., Golewski, P., Knec, M., 2013, Modern Hybrid Joints in Aerospace: Modelling and Testing, *Arch Metall Mater*, 58, 163–169.

Sadowski, T., Golewski, P., 2013, Numerical Study of the Prestressed Connectors and Their Distribution on the Strength of a Single Lap, a Double Lap and Hybrid Joints Subjected to Uniaxial Tensile Test, *Arch Metall Mater*, 58, 579–585.

Sadowski, T., Golewski, P., Zarzeka-Raczkowska, E., 2011, Damage and Failure Processes of Hybrid Joints: Adhesive Bonded Aluminium Plates Reinforced by Rivets, *Comp Mater Sci*, 50, 1256–1262.

Sun, Y.F, Shen, J.M, Morisada, Y., Fujii, H., 2014, Spot friction stir welding of low carbon steel plates preheated by high frequency induction, *Mater Design*, 54, 450–457.

Venukumar, S., Yalagi, S., Muthukumaran, S., 2013, Comparison of Microstructure and Mechanical Properties of Conventional and Refilled Friction Stir Spot Welds in AA 6061-T6 Using Filler Plate, *T Nonferr Metal Soc*, 23, 2833–2842.

Yuan, W., Mishra, R.S, Webb, S., Chen, Y.L, Carlson, B., Herling, D.R., Grant, G.J, 2011, Effect of Tool Design and Process Parameters on Properties of Al Alloy 6016 Friction Stir Spot Welds, *J Mater Process Tech*, 211, 972–977.

Zhang, Z., Zhang, H.W, 2009, Numerical Studies on Controlling of Process Parameters in Friction Stir Welding, *J Mater Process Tech*, 209, 241–270.

ANALIZA NUMERYCZNA PUNKTOWYCH POŁĄCZEŃ ZGRZEWANYCH TARCIOWO Z MIESZANIEM MATERIAŁU

Streszczenie

W pracy przedstawiono analizę rozciągania próbek ze stopu aluminium 6061-T6. Trzy rodzaje próbek powstały poprzez połączenie za pomocą punktowego zgrzewania tarciowego z mieszaniem materiału. Każda z próbek składała się z jednej zgrzeiny łączącej dwie blachy, różniące się ustawieniem. W pierwszej kąt pomiędzy blachami wynosił 0^o, w celu wyznaczenia nośności połączenia na rozciąganie. W drugiej i trzeciej, kąt wynosił 20^o i -20^o. Takie ustawienie blach pozwala na określenie maksymalnej siły i przemieszczenia struktury rozciąganej i skręcanej. Analizy numerycznej dokonano za pomocą oprogramowania ADINA System opartego na Metodzie Elementów Skończonych (MES). Blachy oraz zgrzeiny zamodelowano jako elementy 3D-solid. Badania eksperymentalne przeprowadzono z wykorzystaniem bezkontaktowego oraz nieingerującego w materiał systemu pomiarowego, stosowanego do badań obciążonych struktur w celu wyznaczenia trójwymiarowych przemieszczeń, odkształceń powierzchniowych. Analizowano rozkład naprężeń, odkształceń oraz przemieszczeń. Dokonano porównania wyników z analizy numerycznej oraz eksperymentu. Struktury rozpatrywano z uwagi na wytrzymałość oraz możliwości zastosowania w przemyśle lotniczym.

Received: September 30, 2014
Received in a revised form: October 27, 2014
Accepted: December 21, 2014